

First Principle Calculation and Data Analysis of Anisotropy in Elastic Properties of Cubic MonoCarbides TiC, VC and NbC

C. Tang¹, J. Guo¹, B. Li¹, A. Kostenevich², L.Wang², G. Rothwell¹ and J. Ren¹

¹ Department of Maritime and Mechanical Engineering, Liverpool John Moores University, Liverpool L3 3AF, UK

² The experimental design-technological office of the E.O. Paton Electric Welding Institute of the National Academy of Sciences of Ukraine

³ School of Engineering, University of Bolton, Bolton BL3 5AB, UK

C.Tang@2015.ljmu.ac.uk; X.J.Ren@ljmu.ac.uk

Abstract. In this work first principle calculation is applied to establish systematic ground state elastic property data of three typical cubic binary monocarbides (TiC, VC and NbC). The bulk modulus, Young's modulus, shear modulus, and Poisson's ratio are determined from the Voigt-Reuss-Hill approximation method and compared with other published data. The micro Vickers hardness is also predicted, the hardness data is compared to published data. The anisotropy in elastic properties of the carbides is studied through calculating the universal elastic anisotropic index; percent anisotropy in compressibility and shear as well as the shear anisotropic factors on the specific crystal planes. A python program is developed to integrate first principle calculation in Materials Studio data and establish the directional anisotropy in elastic properties in 3D space and projection on key crystal planes. 3D constructions and plane projection of the elastic properties based on the maximum, minimum and averaged values approaches is used to present and compare the anisotropy feature of the carbides. The data for E, G and Poisson's ratio is comparatively analysed and discussed, and future direction in developing systematic data through physical modelling is discussed.

Keywords: First Principle Calculation, Carbides, Anisotropy

1. Induction

The ground state structural, elastic, mechanical property data of different carbides (e.g. TiC, VC and NbC) are important for material development and processing. Carbides are widely used in key engineering ceramics and manufacturing tools. Carbides also exist as secondary particles in steels, the structure and properties of which may affect the stiffness, strength, hardness, toughness as well as the grain structures and manufacturability of the material. This is particularly relevant for materials with complex alloying systems such as stainless steels and welded structures. An in-depth understanding of the crystal structures, the mechanical and physical properties of these phases are important for the prediction of their deformation and performance in service. Detailed data of these high melting point phase also relevant to other processes such as nucleation and growth of metallic phases as well as other complex carbides (e.g. Ferrite, Austenite, M_7C_3) [1-3].

First principle calculation is increasingly used in predicting crystal structure, electronic, physical and elastic properties of ceramics (e.g. carbides, nitrides, and multicomponent carbides). First principle calculation is a method to calculate physical properties directly from basic physical quantities (such as the mass and charge, and coulomb force of an electron, etc.) based on the principle of quantum mechanics. It naturally links multidisciplinary research areas and data in physics, chemistry, materials and processing. Typical relevant data from first principles calculation covers elastic constants, physical properties, thermal properties, interface between different phases, electrochemical oxygen Reduction Reaction, corrosion, etc. ([4-6]. The computerised calculation process and subsequent large data analysis generate a rich sources of materials data for establishing more detailed understanding of material parameters and their correlations. For analysis of mechanical properties, the prediction of the elastic properties involves the mathematical approximation combining the Voigt, Reuss and Hill bounds of bulk and shear moduli [7-9]. In addition, the data from first principle calculation and subsequent analysis also provide means to estimate the properties such as Vickers hardness based on the ground state elastic parameters/properties [10-11]. As materials informatics is increasingly being used in engineering analyses and design of complex materials systems, data from physical modelling also offers new opportunities in further understanding of the correlation between different sets of properties with more details. It provides a mean to establish systematic data of the key elastic properties K, E, G, as well as the Poisson's ratio. In addition, by integrating first principle calculation with data analysis, it is possible to establish data for enhancing the understanding and visualization of the difference of properties in different crystal planes or directions. The systematic data in anisotropy is often challenging, or in some cases very difficult, to be established through pure experimental means in particular for secondary particles in steel and welded structures.

In this work as part of a main project in developing data led approach in advanced steels and welded structures, first principle calculation is used to establish systematic data of three typical cubic binary

monocarbides (TiC, VC and NbC). The key elastic constants are obtained from the first principle calculation. The bulk modulus, Young's modulus, shear modulus, and Poisson's ratio are determined from the Voigt-Reuss-Hill approximation method and compared with other published data. The micro Vickers hardness is also predicted and compared to published data. The anisotropy in elastic properties of the carbides is studied through calculating the universal elastic anisotropic index; percent anisotropy in compressibility and shear as well as the shear anisotropic factors on the specific crystals planes. A python based program is developed and used to integrate first principle calculation (using Materials Studio CASTEP) and data processing to establish the elastic properties in 3D space and projection on key crystal planes. The plane projection of the elastic properties on the (001) plane based on the maximum, minimum and averaged values approaches is used to present and compare the anisotropy feature of the carbides. The data for E, G and Poisson's ratio is comparatively analysed and discussed, and future direction in developing systematic data through physical modelling is discussed.

2. Computational Method and data integration

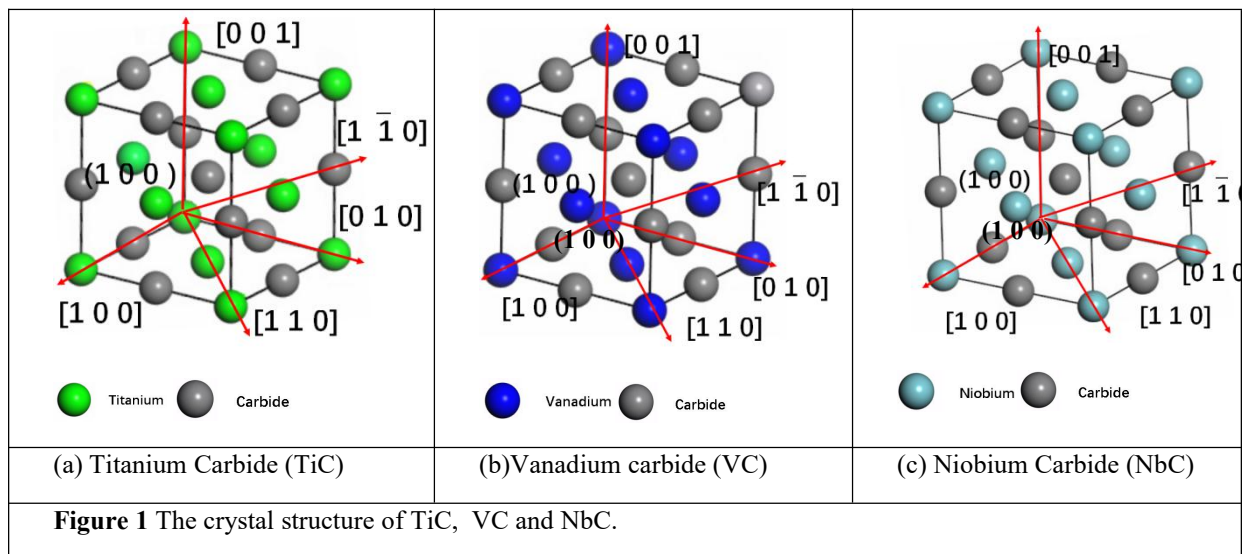


Figure 1 shows the crystal structures of carbides TiC, VC and NbC. TiC is a binary carbides of group VI metal, while the VC and NbC are binary carbides of Group V metal. These carbides are widely used in making key engineering ceramics. In addition, as secondary phases, their structures and properties are also critical for high alloy steels and welded structures. It affects the strength, hardness and thermal stability, as well as the microstructures (e.g. the nucleation of ferrite/austenite). These carbides were also reported to have refinement functions on other more complex multicomponents carbides systems such as $M(\text{Fe,Cr})_7\text{C}_3$ carbides [12]. All these three carbides follow a cubic structure. The carbide for Ti has only one main form (TiC) while Niobium and Vanadium may form carbide of different formulas and compositions (NBC and NB_2C for Nb; V_8C_7 , V_6C_5 , V_4C_3 , V_5C_3 , V_2C for V)[13-14]. The results presented in this paper is focused on data for the simple form of the carbides and anisotropy in the elastic properties analyzed through general anisotropy index and directional anisotropy through 3D surface configuration and plane projections.

Figure 2 shows the data flow and main works integrating the calculation in Materials studio CASTEP, ground state property estimation and anisotropy analysis. Materials Studio CASTEP is an *ab initio* quantum mechanical program that was developed based density functional theory (DFT) to simulate the properties of solids as well as characteristics of interfaces and surfaces. First principle calculation is able to calculate physical properties directly from basic physical quantities (such as the mass and charge, Coulomb force of an electron, etc.) based on the principle of quantum mechanics. As shown in Figure 2, the main functions in the materials studios for calculating the mechanical properties is the geometry optimization and elastic constants prediction, this procedure can optimize the cell size (Lattice parameters) by identifying stable structure with lower total energy. The Generalized gradient approximation (GGA) with Perdew-Burke-Ernzerhof function(PBE) was applied by CASTEP code package. The main data output from the process is the lattice parameters including the lattice constants and the angles. Then the elastic stiffness constants are determined and output in a matrix form. As shown in Figure 2, in the second stage, a python program is developed to calculate the compliance tensors (S_{ij}), which is the derivative of strain with respect to stress. Then the ground state elastic properties are calculated based on the Voigt-Reuss-Hill (VRH) equations [15]. The theoretical hardnesses of the carbides are also determined from the bulk and shear modulus. The general anisotropic index of the crystal is calculated, which represents the difference in the values of K, G and E. The data is a generalised property without considering the

actual anisotropy at directions. In the third part, a more complex program and data analysis is performed to plot the elastic properties in spherical coordinates to visualise the data of K, G, E and ν in 3D, which provides a mean to analyse the directional anisotropy in E, G and Poisson's ratio and their projections on key crystal planes. This provide a more detailed way to quantify and visualise the anisotropy in different elastic properties.

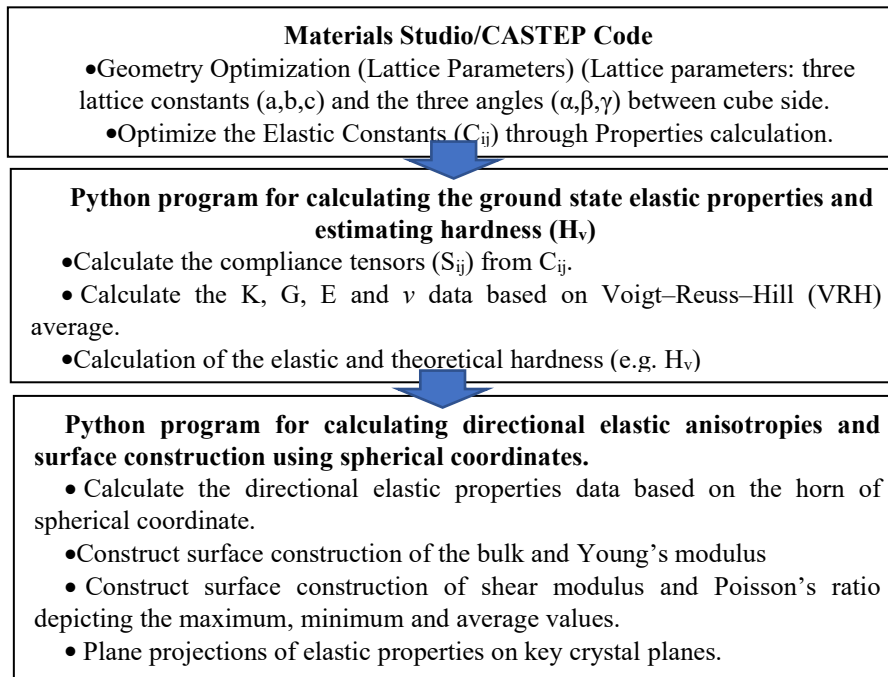


Figure 2 Main programs integrating materials studio and data.

3. Results and analysis

3.1 Elastic constants and ground elastic properties

The elastic constant and structures optimisation were performed in Material Studio. The generalized gradient approximation (GGA) with Perdew–Burke–Ernzerhof function(PBE) was applied by CASTEP code package [15-17]. The key calculation parameters (e.g. the cut-off energy and the k-points) was selected based on systematic convergence analysis. In the test, the cut-off energy and the k-points values were systematically changed until the variation of the energy becomes negligible. The final cut-off energy used is 520V. The SCF tolerance were set as $1e^{-6}$ eV/atom, and for the Brillouin-zone sampling, Monkhorst-Pack mesh was set as $10 \times 10 \times 10$ k-points. One key output data used to calculate the ground state elastic properties are the elastic constants from the CASTEP. It involves calculating stress strain response of the crystal under several different strain patterns based on Hooke's law. Due to symmetry of a cubic crystal, the related elastic constants can be expressed as in Equation (1)

$$\begin{pmatrix} \sigma_1 \\ \sigma_2 \\ \sigma_3 \\ \tau_4 \\ \tau_5 \\ \tau_6 \end{pmatrix} = \begin{pmatrix} C_{11} & C_{12} & C_{12} & & & \\ C_{11} & C_{11} & C_{12} & & & \\ C_{12} & C_{12} & C_{11} & & & \\ & & & C_{44} & & \\ & & & & C_{44} & \\ & & & & & C_{44} \end{pmatrix} \begin{pmatrix} \varepsilon_1 \\ \varepsilon_2 \\ \varepsilon_3 \\ \gamma_4 \\ \gamma_5 \\ \gamma_6 \end{pmatrix} \quad (1)$$

The relationship ($\sigma_i = C_{ij} \varepsilon_j$) is for small stresses. Where σ is the normal stress, τ is the shear stress, ε is the normal strain, γ is the shear strain. The elastic properties of solid material are calculated from stiffness constant C_{ij} (obtained from the first principle calculation) and elastic Compliance Constants S_{ij} [18]. The compliance constants S_{ij} can be determined as the inverse matrix of the elastic stiffness matrix C_{ij} ($[S_{ij}] = [C_{ij}]^{-1}$). As for simple cubic lattice symmetry, there are three independent variables in $[C_{ij}]$ and $[S_{ij}]$, " C_{11} C_{12} , C_{44} " and " S_{11} , S_{12} , S_{44} ", respectively. The Voigt-Reuss-Hill (VRH) approximation is an effective way for converting anisotropic single-crystal elastic constants into effective isotropic (polycrystalline) elastic moduli [19]. The Voigt approach sets the upper bound, the Reuss approach sets the lower bound of the elastic properties while the Hill values takes the average between the Voigt and Reuss predictions[7-9]. The approach provide a mean to

calculate the average properties, the calculation also produce data showing potential difference in properties through comparing the upper and lower limit of the materials properties. Details of the theoretical background can be found in [7-9]. The bulk modulus can be calculated from the elastic constants C_{ij} as:

$$K_v = 2(C_{11} + C_{12} + C_{33}/2 + 2C_{13})/9 \quad (2)$$

$$K_R = 1/[(S_{11} + S_{22} + S_{33}) - 2(S_{12} + S_{23} + S_{31})] \quad (3)$$

$$K_H = (K_V + K_R)/2 \quad (4)$$

The effective shear modulus can be written as:

$$G_V = [(C_{11} + C_{22} + C_{33}) - (C_{12} + C_{23} + C_{31}) + 3(C_{44} + C_{55} + C_{66})]/15 \quad (5)$$

$$G_R = 15/[4(S_{11} + S_{22} + S_{33}) - 4(S_{12} + S_{23} + S_{31}) + 3(S_{44} + S_{55} + S_{66})] \quad (6)$$

$$G_H = (G_V + G_R)/2 \quad (7)$$

The most common equation to estimate the Young's Modulus was based on the Hill bulk modulus (K) and shear modulus (G) with the following equation:

$$E_H = 9K_H G_H / (3K_H + G_H) \quad (8)$$

The effective Poisson's ratio of the crystal can be obtained from bulk modulus and shear modulus. When the Hill model is used, it can be written as:

$$\nu_H = (3K_H - 2G_H) / (6K_H + 2G_H) \quad (9)$$

The Vickers hardness can be calculated following formula for theoretical hardness prediction from the bulk modulus (K) and shear modulus (G) [10-11].

$$\text{Tian's Model: } H_v = 0.92 \left(\frac{G}{K} \right)^{1.137} G^{0.708} \quad (10)$$

$$\text{Chen's Model: } H_v = 2 \left(\left(\frac{G}{K} \right)^{0.585} G \right) - 3 \quad (11)$$

Table 1 Calculated values of bulk modulus (K), Young's modulus (E), shear modulus(G); Poisson's ratio(ν) based on the Reuss, Voigt and Hill models. (the Unit for K, E, G is GPa)

	K(H)	K(V)	K(R)	E(H)	E(V)	E(R)	G(H)	G(V)	G(R)	ν (H)	ν (V)	ν (R)
TiC	252	252	252	427	428	427	175	176	175	0.217	0.217	0.217
VC	306	306	306	501	504	498	204	205	203	0.227	0.226	0.228
NbC	300	300	300	484	493	476	197	201	192	0.23	0.226	0.235

Table 1 lists the key values for K, (G), E and Poisson's ratio(ν) based on the Voigt–Reuss–Hill (VRH) models (Equations 2-9). The averaged values (Hill model) are comparable to published works [20-26]. As shown in the data, the bulk modulus of the crystals determined by the Voigt, Reuss and Hill method are identical, the VC and NbC has much higher compressibility than TiC based on the values of K. The $E_{(v)}$ and $E_{(R)}$ is slightly different for TiC and VC, but there is a clear difference in the Young's modulus of NbC, the Reuss model give a value of 493GPa and the Reuss model give a much lower value of 476 GPa. There is limited difference between the data for the shear modulus between the upper (G(V)) and lower bounds (G(R)) for each of the carbides. The calculated values for the Poisson's ratio ($\nu_{(V)}$, $\nu_{(R)}$, $\nu_{(H)}$) are also similar for each material. Figure 3(a) presents the calculated the bulk modulus, Young's modulus, shear modulus and Poisson's ratio (average values based on the Hill model). The E and G values for VC is slightly higher than that for NbC and TiC. The bulk modulus of NbC is comparable to that of VC, both are higher than the K value of TiC. The Poisson ratio for the carbides are all comparable between the model calculations with the $\nu_{(H)}$ being slightly higher. The predicted data of the modulus shows a good agreement with the published experimental and other theoretical data, for example, TiC [20,21,27]; VC [4, 23]. NbC [24-26]. Other data sources used included matweb (<http://www.matweb.com/>) and CRC Materials Science and Engineering Handbook. Further details can be found in [28]. The Reuss, Voigt and Hill data also provide a mean to estimate the hardness (equations 10 & 11) from the bulk and shear moduli. The data for these carbides is shown in Figure 3(b) together with the range of published data. The different colour (yellow and green) represents the maximum and minimum among the reported values over different sources. It illustrates that, the predicted Vickers hardness values from both models are close to average of published data based on a mix of reference including material data base [e.g. 22, 28, 29].

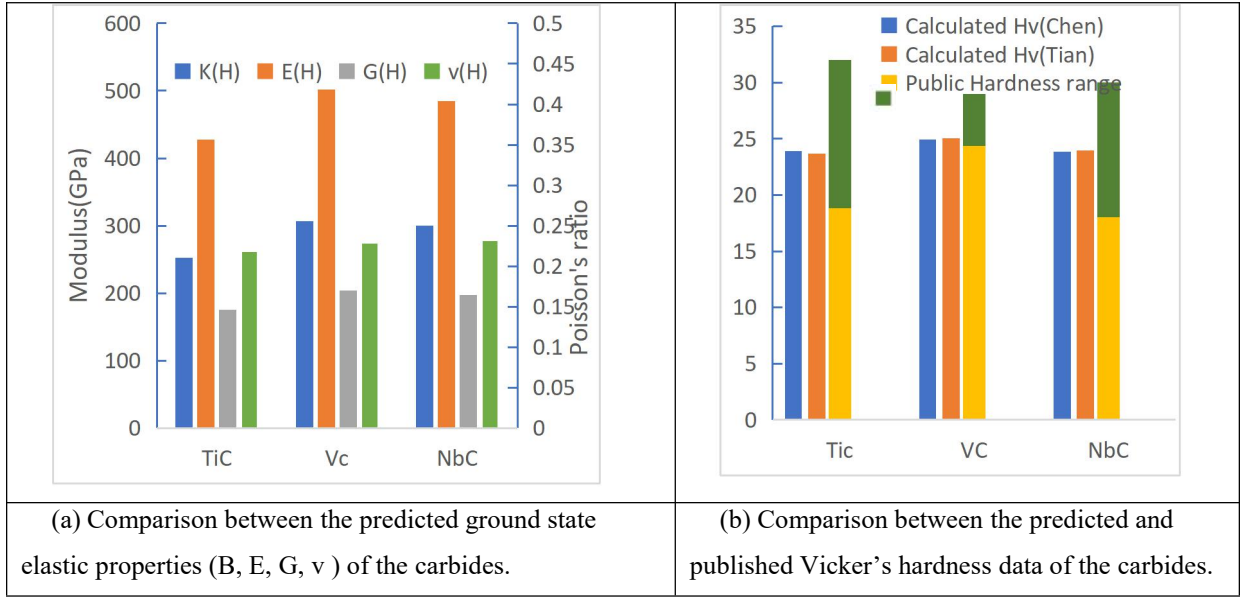


Figure 3 Predicted elastic properties and Vicker's hardness of the carbides.

3.2 Anisotropy in the ground state elastic properties

For ceramics, the anisotropies in elastic properties can influence the formation and propagation of micro cracks and reduce the mechanical durability. The hardness and wear resistance is also related to the anisotropy of the crystal [30]. The anisotropy in crystals are normally represented by anisotropic indexes such as the universal elastic anisotropic index (A_U) [31], percent anisotropy in compressibility and shear (A_{comp} and A_{shear}) [19], and the shear anisotropic factors on the (100), (010), and (001) planes (A_1 , A_2 and A_3) of cubic crystals [32-33]. The equations are:

$$A_U = 5G_V/G_R + K_V/K_R - 6 \quad (12)$$

$$A_{comp} = (K_V - B_R)/(K_V + K_R) \quad (13)$$

$$A_{shear} = (G_V - G_R)/(G_V + G_R) \quad (14)$$

$$\text{For cubic structure, } A_1=A_2=A_3 = A_1 = 4C_{44}/(C_{11} + C_{33} - 2C_{13}) \quad (15)$$

For an elastically isotropic solid, $A_U=A_{Shear}=0$; $A_1=1$. Larger values for A_U and $(1-A)$ indicates more elastic anisotropy.

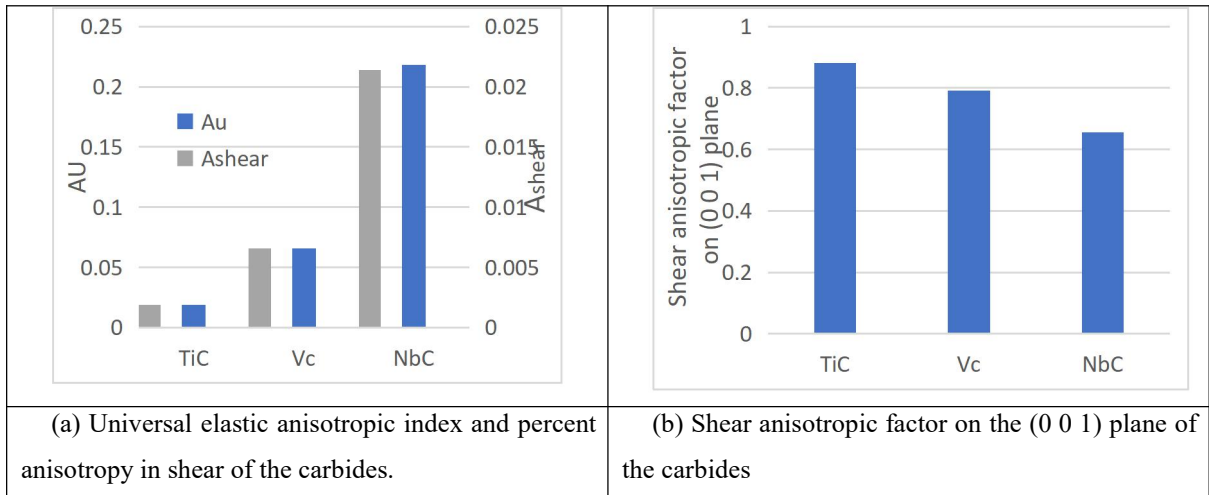


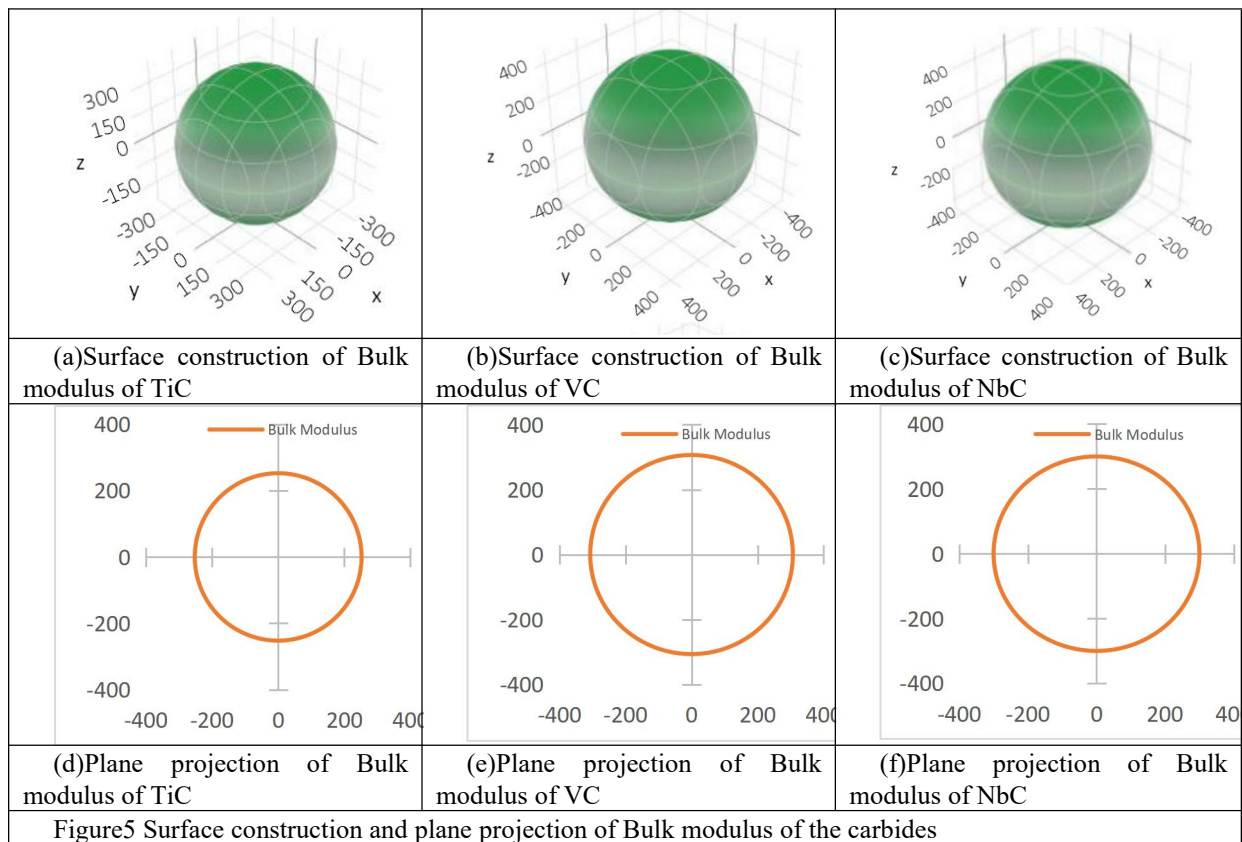
Figure 4 Anisotropy index data of the carbides.

Figures 4a&b plots universal elastic anisotropic index (A_U), percent anisotropy in shear (A_{shear}). It is clearly shown that the A_U for TiC and VC is relatively low with TiC(0.01) and VC (0.066), both are close to isotropic conditions, but NbC has a higher A_U value of 0.21. The values for A_{Shear} of the three carbides are all very low with TiC(0.001), VC(0.006) and NBC(0.021). The shear anisotropic factors on the (001) plane is represented by

the A_1 values (Figure 3d). The values are lower than 1 for all the carbides, indicating anisotropic characteristics on the (100) plane. The A_1 value for TiC is closer to 1, suggesting low anisotropy, VC, NbC shows a much stronger anisotropy with A_1 value of about 0.8 and 0.65, respectively. The data shows that the percent anisotropy in shear (A_{shear}) seems to be a more clearer indicator for anisotropy for the carbides. Both A_U and A_{shear} are generalised value, data for directional anisotropy is required to establish more detailed data and present the anisotropy in a better visualizable way for both materials research, development, teaching and training.

3.3 Directional anisotropy data of elastic properties based on 3D surface construction and plane projection

In order to establish and visualise anisotropy of elastic properties in further details, a python program is developed to calculate the 3D directional distribution of the E, G and Poisson's ratio in spherical coordinate system. The process involves calculating the directional dependence of K, E, G and ν in spherical coordinate to establish the 3D surface construction [15]. Details of the theory can be found in [34] and details of the implementation in Python can be found in [28].



In general, an elastically isotropic solid has a spherical 3D surface construction of elastic parameter. A non-spherical 3D surface construction indicates an elastically anisotropic solid. The more deviation the 3D surface construction from a sphere reflects a higher degree of elastic anisotropy is. [17, 35]. On a crystal plane (e.g. (001)), the degree of anisotropy can be represented by the closeness of the iso line to a circular shape. For cubic structure, the (001), (100) are identical anisotropy. So the data on (001) is representative to the anisotropy feature including maximum and minimum values. Figure 5 shows the surface construction and plane projection of the bulk moduli. For all the carbides, the surface plot of the bulk modulus is spherical, indicating isotropic distribution. This corresponds to the isotropic parameter of compression being '0' (Equation 13).

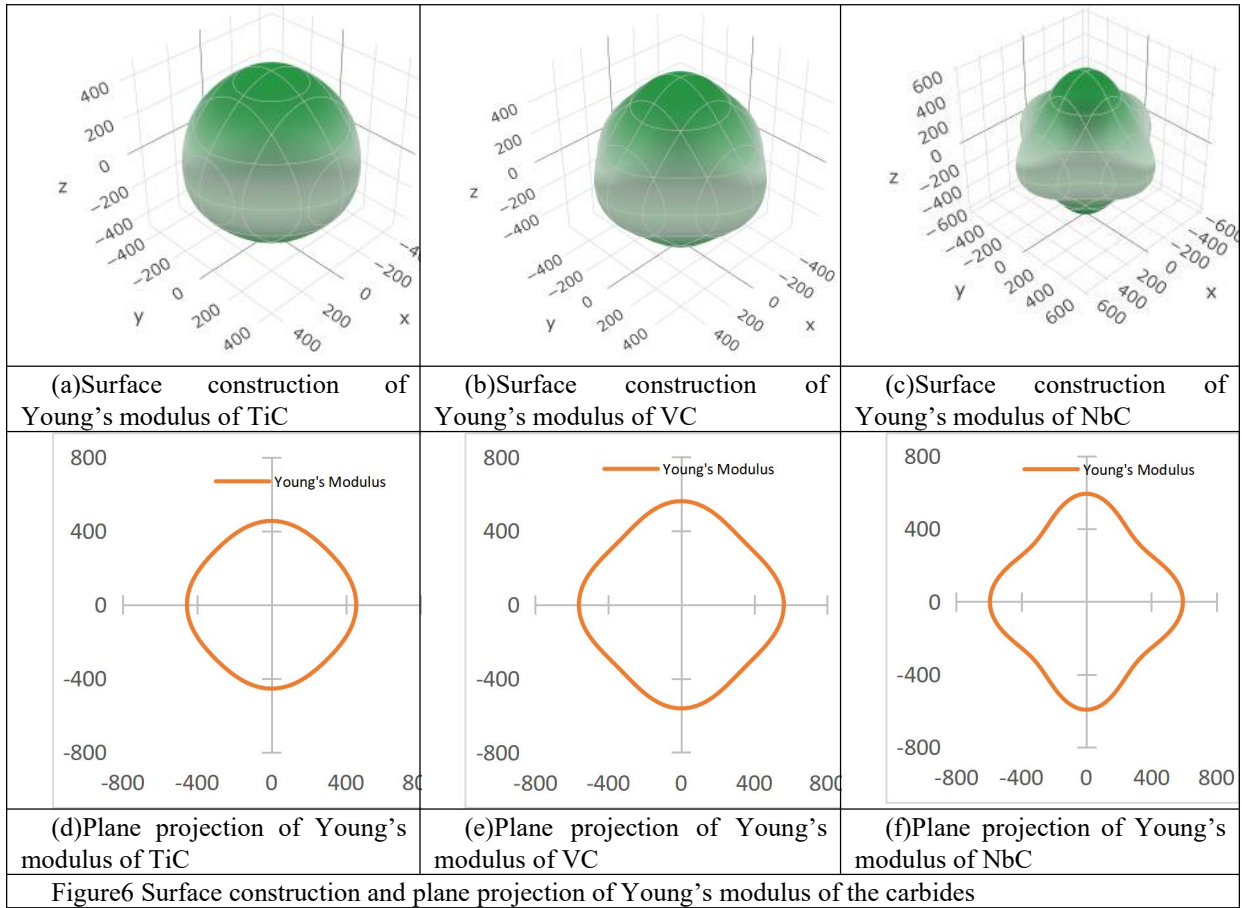
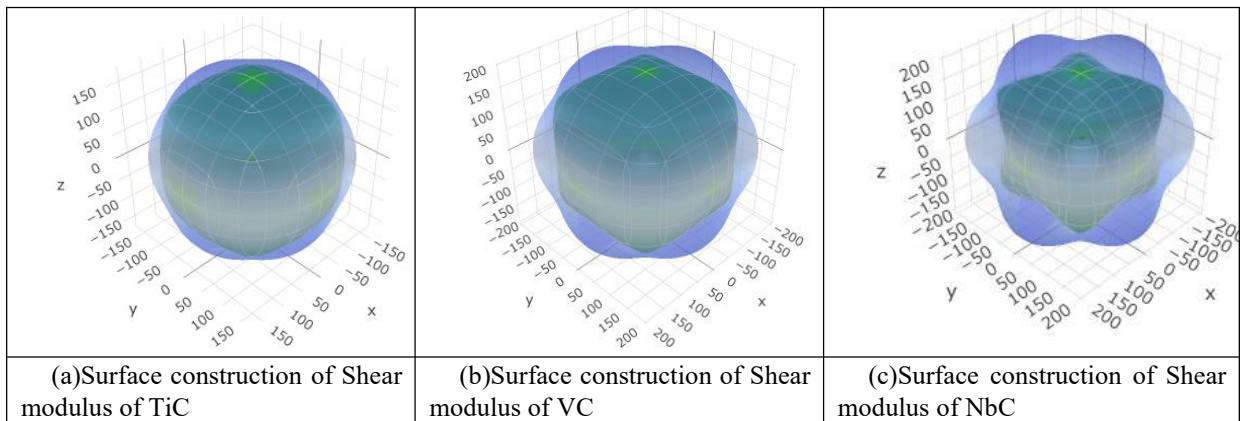


Figure 6 shows 3D surface constructions of Young's moduli for the carbides, which is the main indication of stiffness. The Young's Modulus of TiC has a near-spherical 3D graph, the projection on (100) is approximately circular indicating limited anisotropy. The Young's modulus for VC is deviated away more from near spherical, while the contour for NbC shows significant anisotropy. The plane projection on (001) shows more clearly the directional anisotropy. The data indicate that TiC has limited anisotropy while NbC showed clear visible anisotropy with a high value at [110] direction.



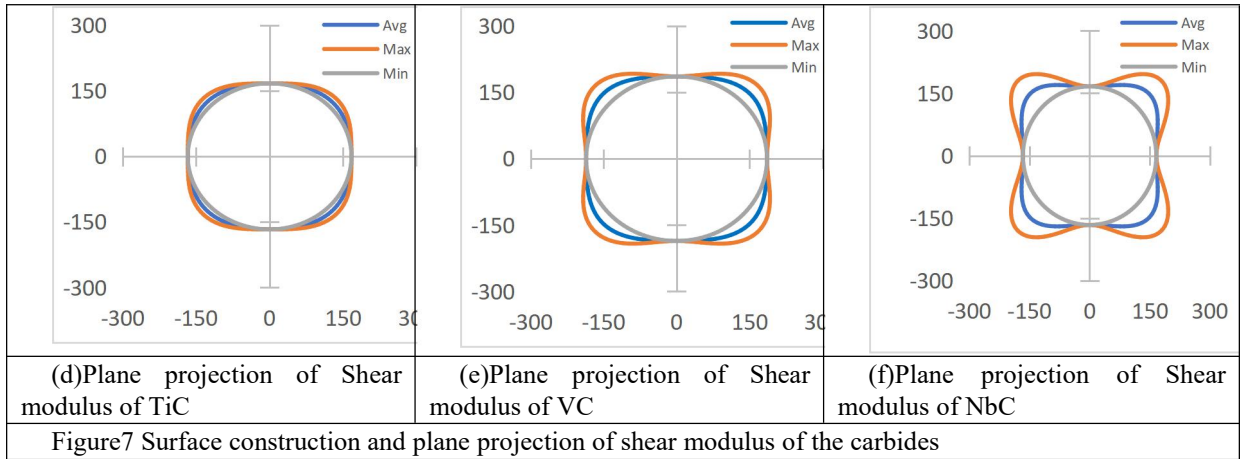


Figure 7 shows the 3D surface constructions and (100) plane projection of the shear moduli of TiC, VC and NbC. Different from the data for the Young's modulus in Figure 6, there are two surface plots (two sets of data), one is based on the maximum value (in Purple) and the other one is based on the minimum values (in green). This reflects the complex nature of the plane and direction of the shear modulus [31]. The 3D construction of G for TiC is close to a spherical shape indicating isotropic, the surface for VC shows some increased anisotropy as the shape of the 3D surface is deviated from a perfect spherical shape. The shear modulus of NbC shows a stronger anisotropic, but the scale of anisotropic is not as significant as that for the Young's Modulus. The plane projections of shear modulus show the anisotropy more clearly as shown in Figures 7 (d,e,f) based on the isolines of the maximum values (in orange); minimum values (in grey line) and an isoline representing the average value (in blue). This approach could indicate more clearly the nature and scale of anisotropy. The isolines on the plane projection shows clearly that the higher G values are at the $[110]$ direction.

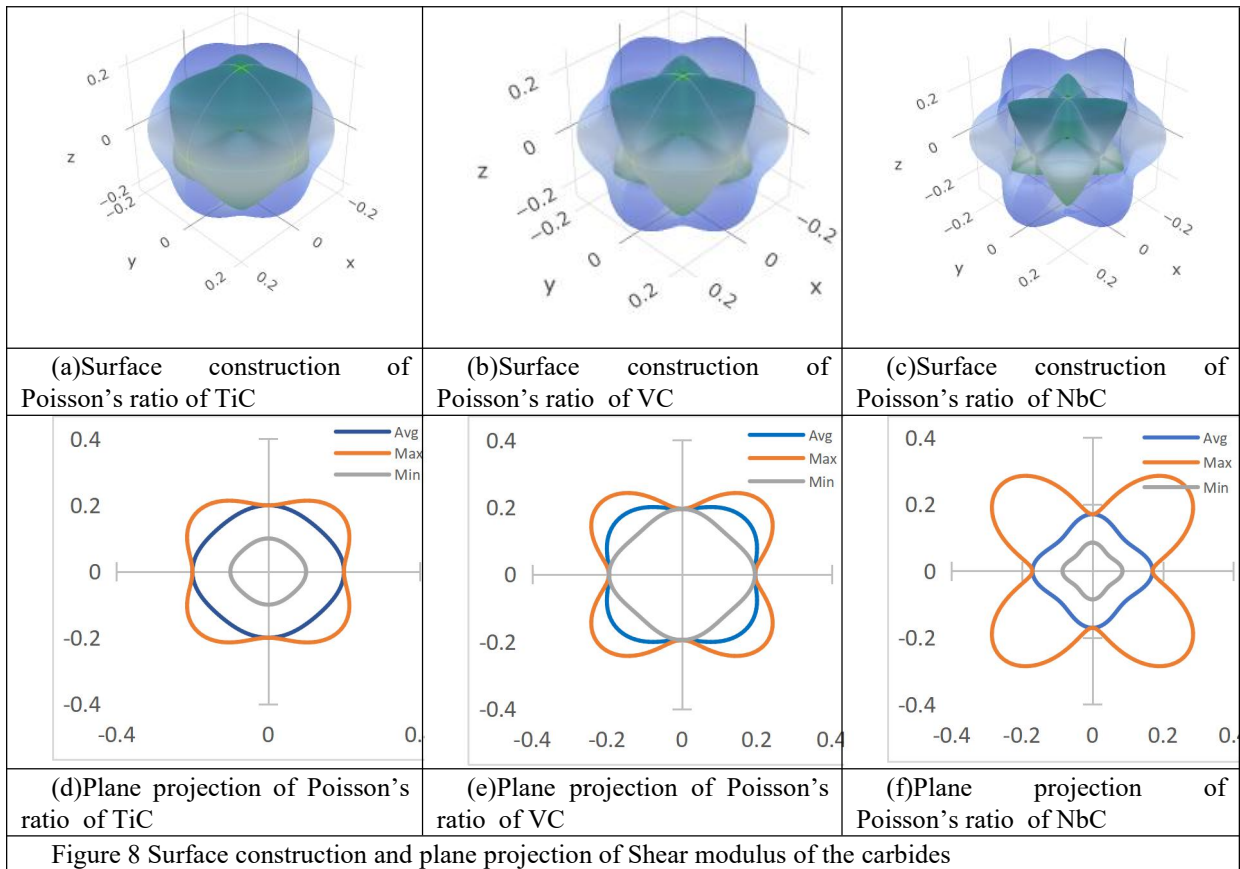


Figure 8 shows 3D surface constructions and plane projection of Poisson's ratio of TiC, VC and NbC. The same colour code and approach is used for presenting the anisotropy in the Poisson's ratio. In general, all the

three carbides showed clear anisotropy in the Poisson's ratio, a much higher Poisson's ratio exist in [110] direction.

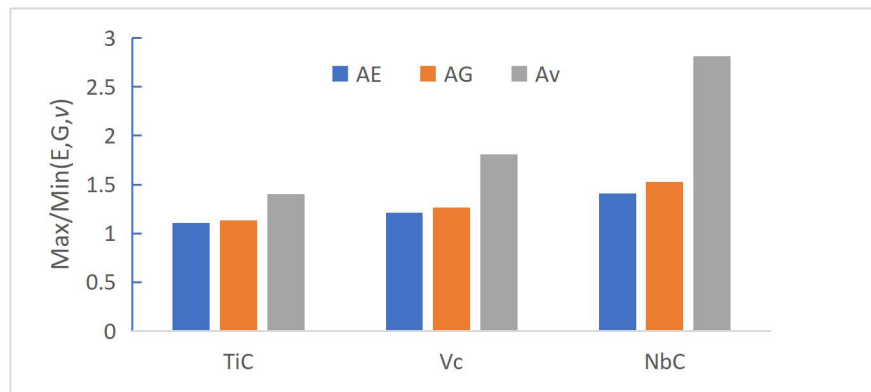


Figure 9 Anisotropy in elastic properties(E, G, ν) based on the ratio between maximum and minimum property value (Max/Min).

Figure 9 plots the ratio between the maximum value and the minimum value of E, G and ν . The data shows a much stronger difference in the data for the Poisson ratio than that for E and G for all the carbides. The scale of anisotropy increased from TiC, VC then NbC. The results showed that 3D construction and plane projection data provide more detailed information than the generalised anisotropy indexes from the Reuss, Voigt and Hill models estimation. The work highlighted the anisotropy nature of the cubic structure carbides in particular in the Poisson's ratio. In general, the anisotropy in these monocarbides are much lower than that of more complex system with the same chemical element system. For example, the A_U for V_2C is as high as over 4 [17]. The integrated approach combining the first principle calculation with python program for anisotropy analysis in particular 3D surface construction and plane projection will help with representing the elastic properties and establishing systematic data at larger scale between different groups of carbides, stoichiometric and non-stoichiometric compounds. The detailed data will also help to quantify the contribution of the Poisson's ratio to materials deformation under complex loading conditions and bring insight to the scatter of property data from different sources. These will be further addressed through meta-data analysis.

4. Conclusion

In this work, first principle calculation is used to establish systematic data of three typical simple cubic binary carbides (TiC, VC and NbC). The bulk modulus, Young's modulus, shear Modulus, and Poisson's ratio are determined from the Voigt-Reuss-Hill approximation together with micro Vickers hardnesses, which shows a good agreement with published experimental data. The anisotropy in elastic properties of the carbides is studied through the universal elastic anisotropic index; percentage anisotropy in shear modulus as well as the shear anisotropic factors on the specific crystal planes. A python based program is developed integrating first principle calculation (Materials Studio) data processing to establish detailed 3D construction of the elastic properties in a spherical coordinates and their projection on key crystal planes. NbC shows a higher anisotropic feature than TiC and VC, and in all the carbides, the Poisson's ratio data showed a stronger anisotropy.

Acknowledgement: This work has received support from the European Union's Horizon 2020 research and innovation program under the Marie Skłodowska-Curie grant agreement No.793114 and No823786.

References:

- [1] Yu, W., Li, J., Shi, C. and Zhu, Q., 2016. Effect of Titanium on the Microstructure and Mechanical Properties of High-Carbon Martensitic Stainless Steel 8Cr13MoV. *Metals*, 6(8), 193.
- [2] Biroasca, S., 2018. *Process-Structure-Property Relationships In Metals*. (Ed.S. Biroasca), Metals
- [3] Xiong, H., Zhang, H., Zhang, H. and Gan, L., 2018. First Principle Calculation of NbC Precipitation Competition between TiC Particle and Ferrite Matrix. *J. Wuhan Univ. Tech.-Mater. Sci. Ed.*, 33(5), 1076-1081.
- [4] Sun, Z., Ahuja, R. and Lowther, J., 2010. Mechanical properties of vanadium carbide and a ternary vanadium tungsten carbide. *Solid State Communications*, 150(15-16), 697-700.
- [5] Cuppari M and Santos S, 2016, Physical Properties of the NbC Carbide, *Metals*, 6(10):250.
- [6] Wen X., Wang Y., Zhao J., 2018 Negatively charged boron nitride nanosheets as apotential metal-free electrocatalyst for the oxygenreduction reaction: a computational study, *New J. of Chemistry* 42(15).
- [7] Voigt.W., 1928, *Handbook of Crystal Physics*, 1928. Leipzig, Taubner.
- [8] Hill.R., 1952, The elastic behaviour of a crystalline aggregate, *Proc. Phys. Soc.* 65, 349.

- [9]Reuss, A., 1929, Calculation of the flow limits of mixed crystals on the basis of the plasticity of monocrystals, *Z. Angew. Math. Mech.* 9, 49–58.
- [10]Chen, X., Niu, H., Li, D. and Li, Y., 2011. Modeling hardness of polycrystalline materials and bulk metallic glasses. *Intermetallics*, 19(9), 1275-1281.
- [11]Tian, Y., Xu, B. and Zhao, Z., 2012. Microscopic theory of hardness and design of novel superhard crystals. *International Journal of Refractory Metals and Hard Materials*, 33, 93-106.
- [12]Chong X, Hua M, Wu P, et al, 2019, Tailoring the anisotropic mechanical properties of hexagonal M7C3 multialloying, *Acta Materialia*, 169, 193-208.
- [13]Hamblyn and Reuben, 1975; Use of Radio-Frequency Plasma in Chemical Synthesis, *Advance in Organic Chemistry and Radio Chemistry/fundamental*, 17, 89-114.
- [14]Wu, L., Yao, T., Wang, Y., et al., 2013. Understanding the mechanical properties of vanadium carbides: Nano-indentation measurement and first-principles calculations. *J. of Alloys and Com.*, 548, 60-64.
- [15]Liu, Y., Chong, X., Jiang, Y. and Feng, J., 2017. Stability, electronic structures, and mechanical properties of Fe–Mn–Al system from first-principles calculations. *Chinese Physics B*, 26(3), p.037102.
- [16]Wang, B., Ma, B., Song, W., Fu, Z. and Lu, Z., 2018. First-principles calculations of structural, electronic, magnetic and elastic properties of Mo₂FeB₂ under high pressure. *Royal Society Open Science*, 5(7), 172247.
- [17]Bao, L., Qu, D., Kong, Z. and Duan, Y., 2019. Anisotropies in elastic properties and thermal conductivities of trigonal TM₂C (TM = V, Nb, Ta) carbides. *Solid State Sciences*, 98, 106027.
- [18]Nye J.F., 1985, *Physical Properties of Crystals*, Oxford University Press, Oxford.
- [19]Chung DH, Buessem WR, in F.W. Vahldiek, S.A. Mersol (Eds.), *Anisotropy in Single Crystal Refractory Compound*, Plenum, New York, 1968.
- [20]Gilman, J. and Roberts, B., 1961. Elastic Constants of TiC and TiB₂. *Journal of Applied Physics*, 32(7), 1405-1405.
- [21]Kim, J and Kang, S., 2012. Elastic and thermo-physical properties of TiC, TiN, and their intermediate composition alloys using ab initio calculations. *Journal of Alloys and Compounds*, 528, 20-27.
- [22]Yang, Y., Lu, H., Yu, C. and Chen, J., 2009. First-principles calculations of mechanical properties of TiC and TiN. *Journal of Alloys and Compounds*, 485(1-2), 542-547.
- [23] Liu, H., Zhu, J., Liu, Y. and Lai, Z., 2008. First-principles study on the mechanical properties of vanadium carbides VC and V₄C₃. *Materials Letters*, 62(17-18), 3084-3086.
- [24]Brown, H., Armstrong, P. and Kempter, C., 1966. Elastic Properties of Some Polycrystalline Transition-Metal Monocarbides. *The Journal of Chemical Physics*, 45(2), 547-549.
- [25]Brenton, R., Saunders, C. and Kempter, C., 1969. Elastic properties and thermal expansion of niobium mono-carbide to high temperatures. *Journal of the Less Common Metals*, 19(3), 273-278.
- [26]Gao, X., Jiang, Y., Liu, Y., Zhou, R. and Feng, J., 2014. Stability and elastic properties of Nb_xC_y compounds. *Chinese Physics B*, 23(9), 097704.
- [27]Török E, Perry A.J., Chollet L. and Sproul W.D., 1987, Young's modulus of TiN, TiC, ZrN and HfN, *Thin Solid Films*, 153, 26, 37-43.
- [28]Tang C., 2020, Ph.D. Thesis, Liverpool John Moores University, UK.
- [29]Edström, D., Sangiovanni, D., Hultman, L., Petrov, I., Greene, J. and Chirita, V., 2018. Elastic properties and plastic deformation of TiC- and VC-based pseudobinary alloys. *Acta Materialia*, 144, pp.376-385.
- [30]Ren XJ, Hooper R. M., Griffiths C., Henshall J. L., 2002, Indentation-size effects in single-crystal MgO, 2001. *Philosophical Magazine A*, 82, 10.
- [31]Ranganathan SI and Ostoja-Starzewski M, 2008, Universal Elastic Anisotropy Index, *Physical Review Letters* 101(5):055504.
- [32]Ravindran P., Fast L., Korzhavyi PA, Johansson B, 1998, Density functional theory for calculation of elastic properties of orthorhombic crystals: Application to TiSi₂, *J Appl Phys*, 1998, 84(9), 4891.
- [33]Liu, X., Feng, Q., Tang, B., et al., 2019. First-principles calculations of mechanical and thermodynamic properties of tetragonal Be₁₂Ti. *RSC Advances*, 9(10), 5302-5312.
- [34]Luan X, Qin H, Liu F, Dai Z, Yi Y, and Li Q, 2018, The Mechanical Properties and Elastic Anisotropies of Cubic Ni₃Al from First Principles Calculations, *Crystals* 2018, 8, 307.
- [35]Sun, S., Fu, H., Lin, J., et al. 2017. The stability, mechanical properties, electronic structures and thermodynamic properties of (Ti, Nb)C compounds by first-principles calculations. *J. of Materials Research*, 33(4), 495-506.